Electronic Supplementary Material (ESI) for Journal of Materials Chemistry A.

Rationally Regulating the Terminal Unit and Copolymerization Spacer of Polymerized Small-molecule Acceptor for All-polymer Solar Cells with High Open-circuit Voltage over 1.10 V

Tao Jia,[‡ab] Jiabin Zhang,[‡a] Guanglong Zhang,[b] Chunchen Liu,[a] Haoran Tang,[a] Kai Zhang*[a] and Fei Huang*[a]

[a] *Institute of Polymer Optoelectronic Materials and Devices, State Key Laboratory of Luminescent Materials and Devices, South China University of Technology, Guangzhou 510640, China.*
[b] *School of Optoelectronic Engineering, Guangdong Polytechnic Normal University, Guangzhou, 510665, China.*

[*] *Corresponding author*
E-mail: mszhangk@scut.edu.cn (K. Zhang); msfhuang@scut.edu.cn (F. Huang)

[‡] *These authors contributed equally to this work.*

Experimental Section

Materials

Compound 12,13-bis(2-decyltetradecyl)-3,9-diundecyl-12,13-dihydro-[1,2,5]thiadiazolo[3,4-e]thieno[2",3":4',5']thieno[2',3':4,5]pyrrolo[3,2-g]thieno[2',3':4,5]thieno[3,2-b]indole-2,10-dicarbaldehyde (TPT-DT-CHO) and polymer donor JD40 were synthesized according to our previous works [1,2]. Compound 4-bromo-3,6-difluorophthalic acid **(1)**, 2,5-Bis(trimethylstannyl)thiophene (DSn-Th) and 5,5'-bis(trimethylstannyl)-2,2'-bithiophene (DSn-DTh) were purchased from Solarmer Materials Inc. Other chemicals and solvents are purchased from Sigma, Alfa Aesar and TCI Chemical Co. and used as received.

Synthetic Procedures

Synthesis of 5-bromo-4,7-difluoro-1H-indene-1,3(2H)-dione (FFOBr).

4-Bromo-3,6-difluorophthalic acid (compound 1) (28.1, 0.1mol) was added into a dried round flask (250 mL) with 150mL acetic oxide. The mixture was stirred at 120 ^{o}C for 12 hours. After being cooled to room temperature, the organic solvent was removed by evaporation at reduced pressure and afforded the raw product 5-bromo-4,7-difluoroisobenzofuran-1,3-dione (compound 2), which are directly used for the next-step reaction. Compound 2, triethylamine (100 mL), acetic oxide (200 mL) and *tert*-butyl-3-oxopentanoate (20 g) were added to a round flask (500 mL) and the mixture was stirred at 65 ^{o}C for 24 hours. After cooled to room temperature, the reaction mixture was poured into hydrochloric acid (5M). The precipitate was filtered, washed with water to afford the residue production. The crude product was further recrystallized with diethyl ether to afford compound FFOBr as grayish yellow powder (10.4g, yield 40%). ^{1}H NMR (500 MHz, $CDCl_3$) δ 7.71 (dd, J = 7.4, 4.4 Hz, 1H), 3.31 (s, 2H). MS (m/z): $[M]^+$ calcd. for $C_9H_3BrF_2O_2$, 261.0218; found, 258.9207.

Synthesis of (2E,2'E)-2,2'-((12,13-bis(2-decyltetradecyl)-3,9-diundecyl-12,13-dihydro-[1,2,5]thiadiazolo[3,4-e]thieno[2",3":4',5']thieno[2',3':4,5]pyrrolo[3,2-g]thieno[2',3':4,5]thieno[3,2-b]indole-2,10-diyl)bis(methaneylylidene))bis(5-bromo-4,7-difluoro-1H-indene-1,3(2H)-dione) (M-FFOBr)

Compound TPT-DT-CHO (2 mmol), compound FFOBr (7 mmol), triethylamine (2 mL) and chloroform (100 mL) were added into a two-neck flask under nitrogen atmosphere. The mixture was stirred at 65 ^{o}C for 18 hours. After being cooled to room temperature, the crude mixture was straightway purified with column chromatography on silica gel using PE /DCM (1.5/1, *v/v*) as the

eluent to afford compound M-FFOBr as black solid (3.376g, 86% yield). ^{1}H NMR (500 MHz, $CDCl_3$) δ 8.21 (d, *J* = 9.3 Hz, 2H), 7.74 – 7.50 (m, 2H), 4.78 (m, 4H), 3.21 (t, *J* = 7.3 Hz, 4H), 2.18 (m, 2H), 1.91–1.85 (m, 4H), 1.51–1.46 (m, 4H), 1.38 (m, 4H), 1.28 – 1.21 (m, 28H), 1.17 – 1.12 (m, 36H), 1.04 – 0.98 (m, 36H).0.87 – 0.80 (m, 22H).^{13}C NMR (126 MHz, $CDCl_3$): δ 185.26, 185.01, 184.96, 184.71, 154.37, 153.94, 152.24, 152.00, 151.81, 151.72, 150.11, 149.63, 147.43, 144.62, 144.61, 137.63, 137.60, 137.56, 135.86, 134.39, 134.36, 133.65, 133.59, 133.56, 133.50, 132.70, 132.69, 129.58, 129.51, 129.45, 129.38, 128.07, 127.96, 127.59, 127.39, 127.27, 127.16, 126.89, 126.78, 126.20, 126.09, 119.70, 119.68, 119.66, 118.19, 118.13, 117.98, 117.80, 117.74, 113.31, 113.30, 55.61, 39.05, 39.02, 31.96, 31.93, 30.93, 30.46, 29.83, 29.71, 29.67, 29.64, 29.58, 29.45, 29.41, 29.36, 25.57, 25.53, 22.70, 14.12. MALDI-TOF-MS (m/z): $[M]^+$ calcd. for $C_{108}H_{148}Br_2N_4O_4S_5$, 1962.498; found, 1962.817.

The universal synthetic procedures for PFFO-Th and PFFO-DTh

Monomer M-FFOBr (196.2mg, 0.1 mmol), 2,5-Bis(trimethylstannyl)thiophene (DSn-Th) (41mg, 0.1 mmol) or 5,5'-bis(trimethylstannyl)-2,2'-bithiophene (DSn-DTh) (49.2mg, 0.1 mmol), $Pd_2(dba)_3$ (1.8 mg) and P (*o*-tol)$_3$ (2.7 mg) were combined in a 15 mL sealed tube. Dry chlorobenzene (CB) (5 mL) was added under argon atmosphere. The mixture was reacted at 110 ^{o}C for 72 h. After cooled down to room temperature, the reactant mixture was poured into MeOH (200 mL). The precipitate was filtered and Soxhlet extracted with methanol, hexane, chloroform. The ingredient extracted from chloroform was concentrated, precipitated into 200 mL methanol, filtered and dried under vacuum to give the dark solid: PFFO-Th (yield 76 %, M_n = 15.4 kDa, M_w = 29.8 kDa); PFFO-DTh (yield 72 %, M_n = 12.6 kDa, M_w = 30.0 kDa).

Instruments and Measurement

^{1}H NMR and ^{13}C NMR spectra were measured on a Bruker AV-500 MHz spectrometer with tetramethylsilane (TMS) as the internal reference. Mass spectra were measured on Bruker ultrafleXtreme or Bruker tims-TOF. Molecular weights of the polymers were obtained on an Acquity Advanced Polymer Chromatography (Waters) with high temperature chromatograph, using 1,2,4-trichlorobenzene as the eluent at 150 ^{o}C. UV-Vis absorption spectra were recorded on a SHIMADZU UV-3600 spectrophotometer. Photoluminescence (PL) was measured with a HORIBA FLUOROMAX-4 fluorimeter. Cyclic voltammetry (CV) was measured on a CHI660e Electrochemical Workstation equipped with a glass carbon working electrode, a platinum wire counter electrode, and a saturated

calomel reference electrode. The potential of saturated calomel electrodes (SCE) was internally calibrated as 0.39 V by using the ferrocene/ferrocenium redox couple (Fc/Fc^+), which has a known reduction potential of –4.80 eV. The scan rate is 50 mV/s. Tapping-mode atomic force microscopy (AFM) images were obtained by using a Bruker Multimode 8 Microscope. Transmission electron microscopy (TEM) images were obtained using a JEM-2100F instrument. Grazing-incidence wide-angle X-ray scattering (GIWAXS) was measured at 13A beam line of National Synchrotron Radiation Research Center (NSRRC, Taiwan)，and were provided technical support by "Ceshigo Research Service，www.ceshigo.com". All samples for GIWAXS were radiated at 12 keV X-ray with an incident angle of 0.12°. The DFT calculations was performed at B3LYP/6-31+G(d,p) level using the Gaussian 16 suite of programs.

The hole-only and electron-only devices were fabricated with the architectures of ITO/PEDOT:PSS/active layer/MoO_3/Ag and ITO/ZnO/active layer/PNDIT-F3N-Br/Ag, respectively. Hole-only and electron-only devices were recorded with a Keithley 236 sourcemeter under dark. The hole and electron mobilities were determined by fitting the dark current to the model of single-carrier SCLC, which is described by the equation,

$$J = \frac{9}{8}\varepsilon_0\varepsilon_r\mu\frac{V^2}{d^3}$$

where J is the current density, μ is the zero-field mobility, ε_0 is the permittivity of free space, ε_r is the relative permittivity of the material, d is the thickness of the active layers, and V is the effective voltage. The effective voltage was obtained by subtracting the built-in voltage (V_{bi}) and the voltage drop (V_s) from the series resistance of the whole device except for the active layers from the applied voltage (V_{appl}), $V = V_{appl} - V_{bi} - V_s$. The hole and electron mobilities can be calculated from the slope of the $J^{1/2}$-V curves.

Device Fabrication and characterization

The conventional structure of ITO/PEDOT:PSS/active layer/PNDIT-F3N-Br/Ag was used to fabricate the all-PSCs devices. The indium tin oxide (ITO) substrates were cleaned by sequentially sonication with detergent, deionized water, and isopropanol. After dried in oven at 80 °C overnight, the substrates were treated with an oxygen plasma for 5 min and then coated with PEDOT:PSS (CLEVIOS PVP Al 4083) at 3500 rpm for 30 s. Annealing at 150 °C on a hot plate in air for 15 min gave a thin film of about ～40 nm. Then the substrates were transferred into a N_2 protected glove box. The active

layers were obtained by spin-coating the CF blend solution containing chloronaphthalene additive with a total concentration of 8 mg mL^{-1}. The optimal film thickness of ca. 100 nm was obtained by controlling the rotate speed of ~2300 rpm. The film thicknesses were measured with a Bruker AXS Dektak stylus surface profiling system. All the active layers were thermal annealed in a hot plate for 10 min. Subsequently, ~10 nm PNDIT-F3N-Br (dissolved in methanol, 1 mg mL^{-1}) as cathode interface was spin-coated onto the active layers. Finally, 100 nm Ag were thermally deposited on top of the interface through a shadow mask in a vacuum chamber at a pressure of 3×10^{-7} torr. The effective area of the device was confined as 0.04 cm^2 by a non-refractive mask to improve the accuracy of measurements. The current density−voltage ($J-V$) characteristics were measured under a computer controlled Keithley 2400 sourcemeter under 1 sun, AM 1.5G solar simulator (Taiwan, Enlitech SS-F5). The light intensity was calibrated by a standard silicon solar cell (certified by NREL) before the testing, giving a value of 100 mW cm^{-2} during the test of $J-V$ characteristics. The external quantum efficiency (EQE) spectra were recorded with a QE-R measurement system (Enlitech, QE-R3011, Taiwan).

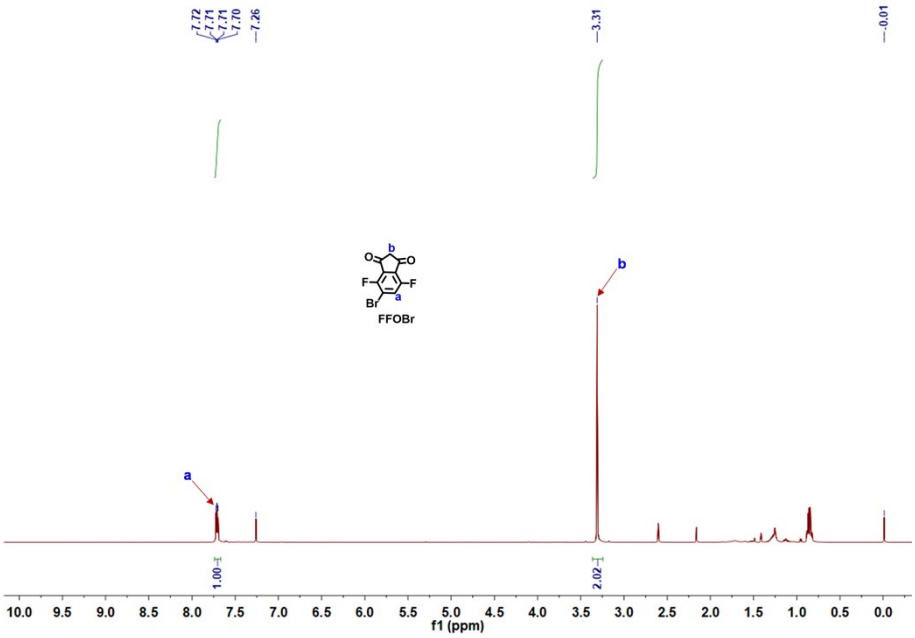

Figure S1. ^1H NMR spectrum of FFOBr in $CDCl_3$.

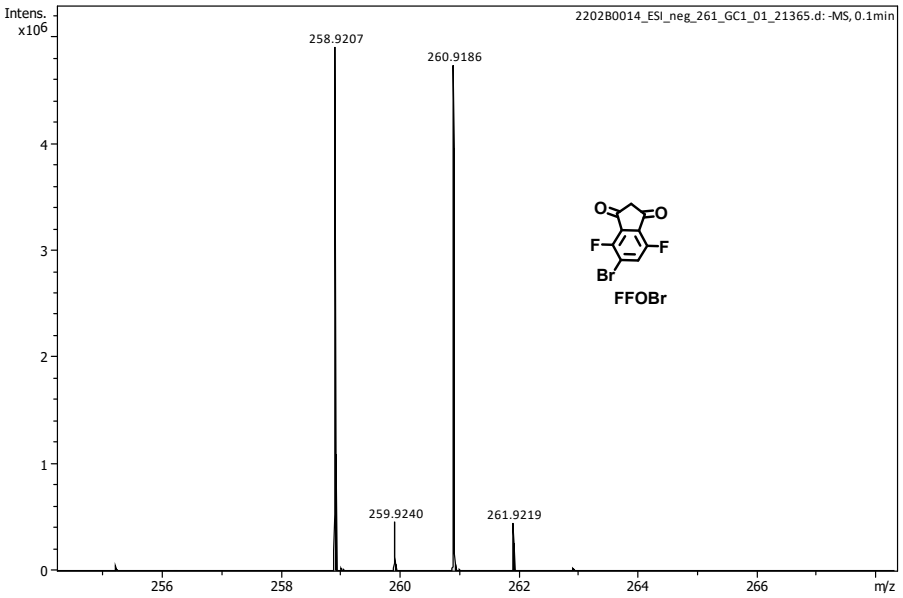

Figure S2. ESI-Mass spectrum of FFOBr terminal unit.

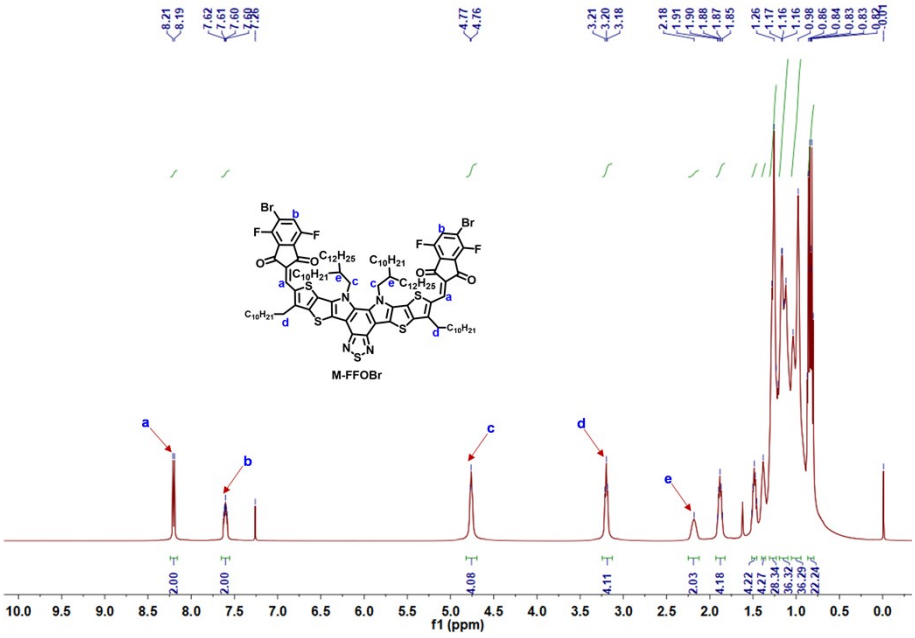

Figure S3. ^{1}H NMR spectrum of M-FFOBr in $CDCl_3$.

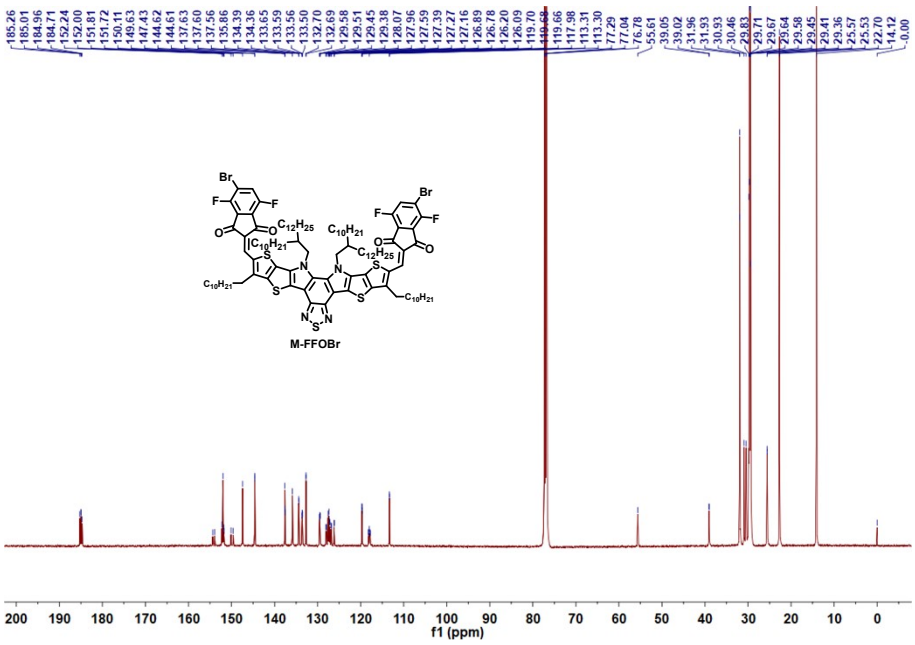

Figure S4. ^{13}C NMR spectrum of M-FFOBr in $CDCl_3$.

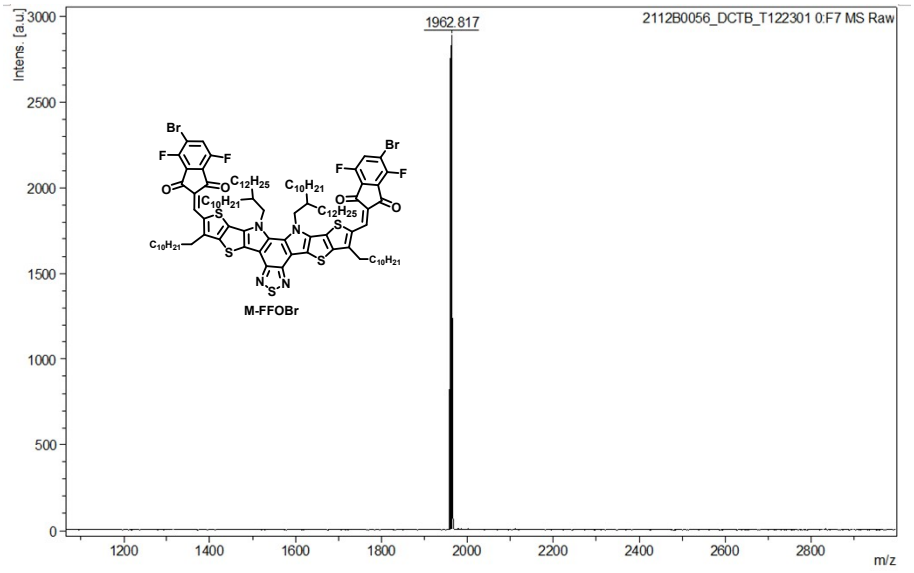

Figure S5. MALDI-TOF-mass spectrum of M-FFOBr.

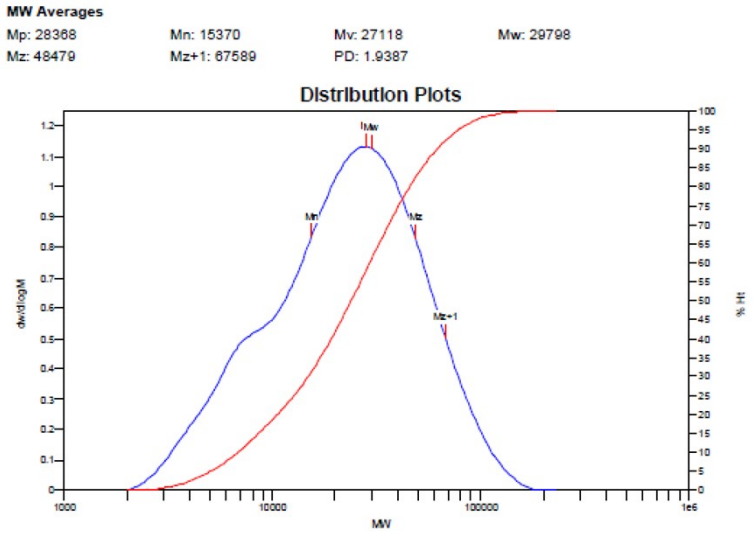

Figure S6. High-temperature GPC measurements of PFFO-Th.

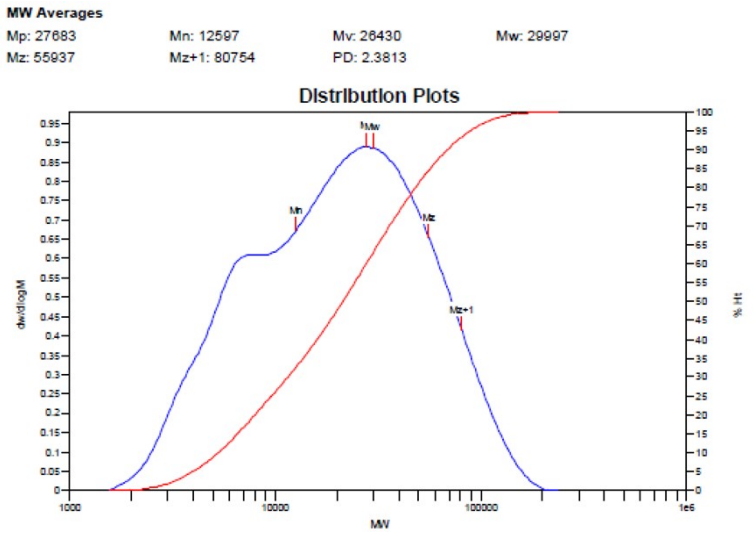

Figure S7. High-temperature GPC measurements of PFFO-DTh.

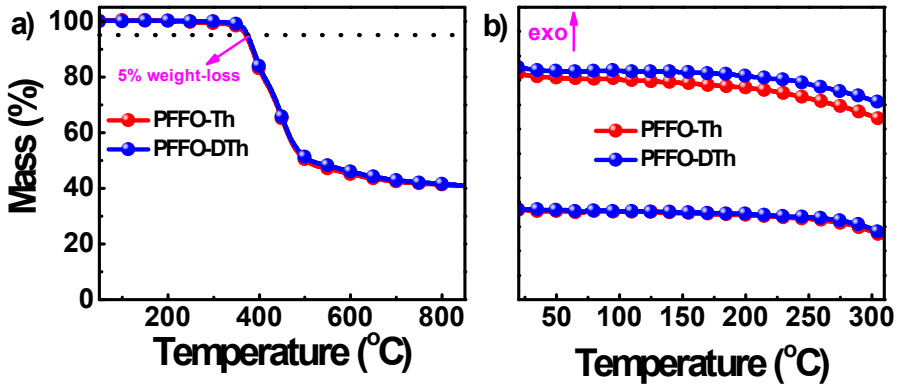

Figure S8. (a) Thermogravimetric (TG) and (b) differential scanning calorimetry (DSC) characteristics.

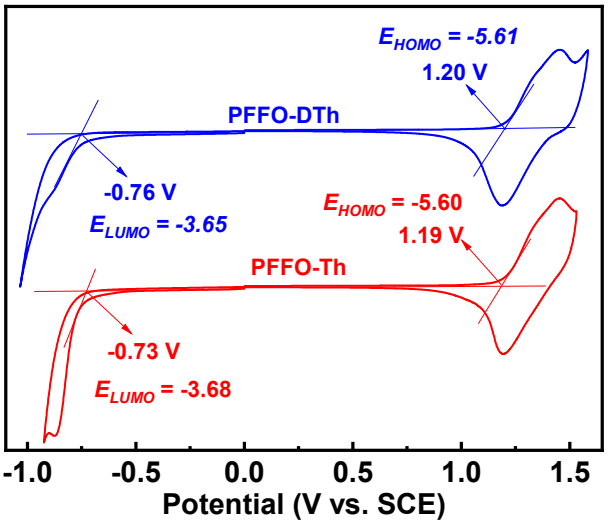

Figure S9. CV characteristics of PFFO-Th and PFFO-DTh.

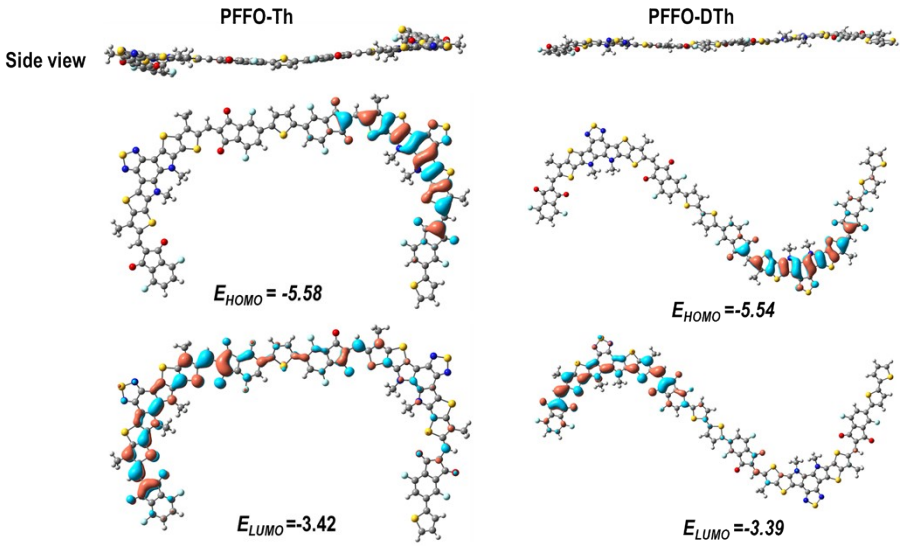

Figure S10. Optimized conformations and molecular orbitals of the molecular models with two repeat unit of the PSMAs based on DFT calculations

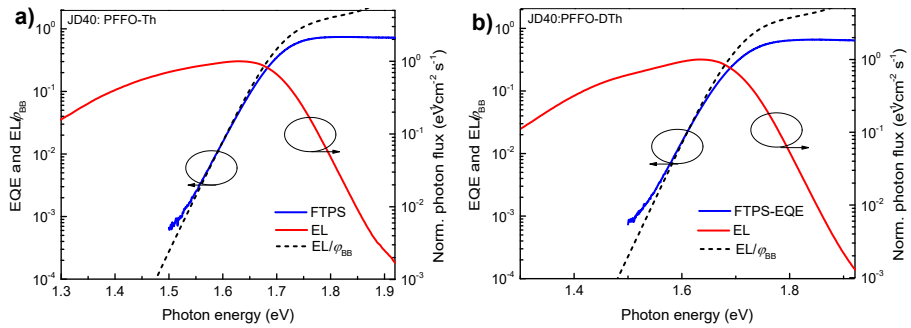

Figure S11. a,b) FTPS-EQE spectra and EQE_{EL} spectra of the all-PSCs based on a) JD40:PFFO-Th and b) JD40:PFFO-DTh.

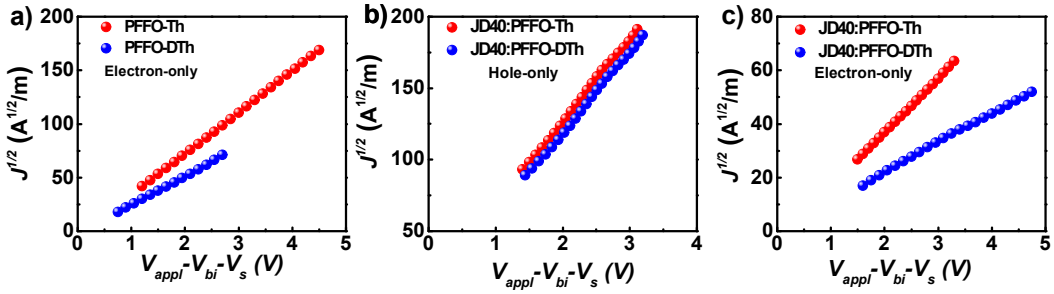

Figure S12. The $J^{1/2}$-V curves of the pristine acceptor and the related blend films.

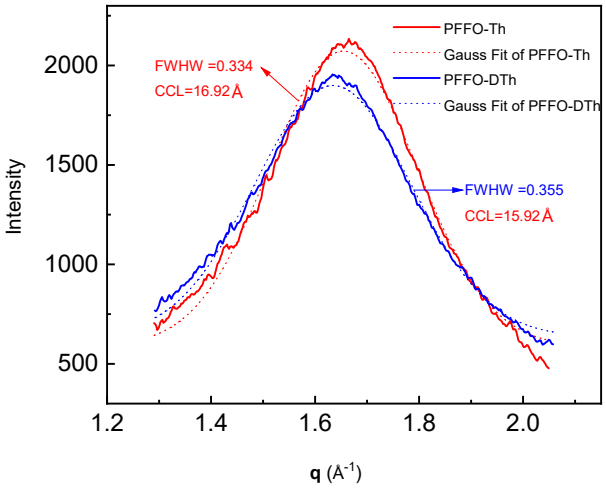

Figure S13. The Gaussian fitting patterns of (010)-OOP direction resulted from the GIWAXS profiles of neat PSMA films.

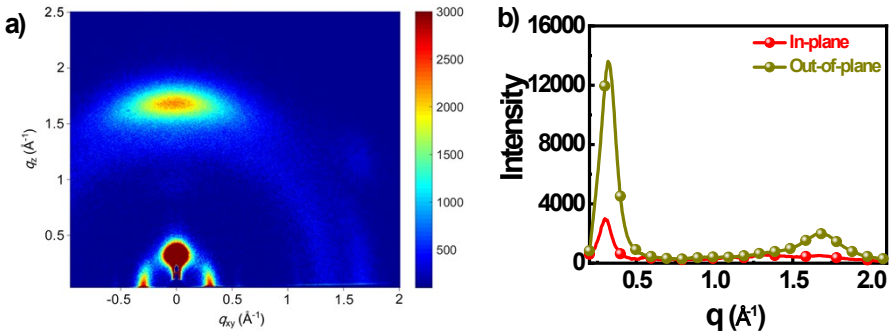

Figure S14. (a) 2D GIWAXS pattern and (b) line-cut curve of polymer donor JD40.

Table S1. Photovoltaic properties of all-PSCs by matching different polymer donors with PFFO-Th.

Polymer donor	V_{oc} (V)	J_{sc} (mA/cm^2)	FF (%)	PCE (%)	PCE_{max} (%)
PM6	1.17±0.01	5.6±0.1	45.9±1.0	3.0±0.1	3.1[a]
PBDB-T	1.08±0.00	12.1±0.1	48.9±0.6	6.4±0.1	6.5[a]

P3HT	0.80±0.00	3.6±0.1	52.1±2.1	1.5±0.1	1.6[a]
JD40-S	1.15±0.00	11.8±0.2	52.1±0.1	7.1±0.1	7.1[a]

[a] with D/A ratio of 1:1, 1% CN additive, processed with CF solvent, with a total concentration of 8 mg mL^{-1};

Table S2. Photovoltaic parameters of all-PSCs based on JD40: PFFO-Th at different D/A weight ratios.

Condition	D/A (*w*/*w*)	V_{OC} (V)	J_{SC} (mA cm^{-2})	FF (%)	PCE (%)	PCE_{max} (%)
CF 8 mg/mL 1%CN	1.5:1	1.10±0.01	14.9±0.3	59.0±2.1	9.7±0.4	10.1
	1.2:1	1.11±0.00	14.6±0.4	62.1±0.7	10.1±0.2	10.3
	1:1	1.11±0.00	15.3±0.1	61.5±0.2	10.5±0.1	10.5
	1:1.2	1.11±0.00	15.3±0.1	62.2±1.3	10.5±0.3	10.8
	1:1.5	1.11±0.01	14.3±0.5	61.3±2.8	9.7±0.3	10.0

Table S3. Photovoltaic parameters of all-PSCs based on JD40: PFFO-Th with different contents of additive.

Condition	CN (%)	V_{OC} (V)	J_{SC} (mA cm^{-2})	FF (%)	PCE (%)	PCE_{max} (%)
CF 8 mg/mL D:A=1:1.2	0.5%	1.09±0.00	15.1±0.2	60.50±0.8	9.9±0.2	10.1
	1%	1.11±0.00	15.3±0.1	62.2±1.3	10.5±0.3	10.8
	2%	1.11±0.00	14.7±0.2	61.0±0.9	10.0±0.1	10.1

Table S4. Detailed energy losses of the all-PSCs based on JD40:PFFO-Th and D40:PFFO-DTh.

Devices	E_g (eV)	q$VOCSQ$ (eV)	q$VOCrad$ (eV)	EQE_{EL}(%)	ΔE_1 (eV)	ΔE_2 (eV)	ΔE_3 (eV)	qV_{OC} (eV)	ΔE_{loss} (eV)
JD40:PFFO-Th	1.70	1.42	1.36	5.5×10^{-3}	0.28	0.06	0.25	1.11	0.59
D40:PFFO-DTh	1.70	1.42	1.36	1.5×10^{-2}	0.28	0.06	0.23	1.13	0.57

Table S5. Hole and electron mobilities of the related pristine and blend films.

AL	μ_h (cm^2 V^{-1} s^{-1})	μ_e (cm^2 V^{-1} s^{-1})	μ_h/μ_e
PFFO-Th	—	4.70×10^{-4}	—
PFFO-DTh	—	1.23×10^{-4}	—
JD40:PFFO-Th	2.48×10^{-3}	3.34×10^{-4}	7.42
JD40:PFFO-DTh	1.86×10^{-3}	7.93×10^{-5}	23.46

References

[1] T. Jia, J. B. Zhang, W. K. Zhong, Y. Y. Liang, K. Zhang, S. Dong, L. Ying, F. Liu, X. H. Wang, F. Huang and Y. Cao, *Nano Energy*, 2020, **72**, 104718.

[2] T. Jia, J. Zhang, K. Zhang, H. Tang, S. Dong, C.-H. Tan, X. Wang and F. Huang, *J. Mater. Chem. A*, 2021, **9**, 8975-8983.